Designing Induced Joints in RCC Arch Dams for Enhanced Crack Prevention: A Contact Unit Simulation and Equivalent Strength Theory Approach

Haifeng Li*

State Key Laboratory of Simulation and Regulation of Water Cycle in River Basin, China Institute of Water Resources and Hydropower Research, 100038 Beijing, China

* Correspondence: Haifeng Li (lihfdlut@126.com)

Abstract: Decades of engineering practice have substantiated that the implementation of construction joints is a pivotal method for mitigating dam cracking. The integration of various joint types, notably transverse and induced joints, within roller-compacted concrete (RCC) arch dams has emerged as a promising strategy to curtail cracking and structural failure. This approach leverages the unique structural characteristics inherent to each joint type. Given the intricate, variable, and dynamic nature of thermal stress in RCC arch dams, the design process for crack prevention, particularly the configuration of induced joints, demands an accurate representation of the dam's operational conditions from construction through to service. Investigations in practical engineering contexts have revealed that the utilization of a contact unit simulation methodology, featuring an open/close iterative function for modeling the behavior of induced and transverse joints in RCC arch dams, proves effective. This method is complemented by the adoption of equivalent strength theory as the criterion for structural integrity assessment. A comprehensive process simulation encompassing the entire dam structure further enhances the efficacy of this approach. Such simulations facilitate a more granular examination of joint placement within the dam and the structural design of the joints themselves. As a result, induced joints can be optimally opened in alignment with design expectations, thereby alleviating tensile stress triggered by temperature reductions. This strategy assures superior construction quality of the dam's concrete body, contributing significantly to the longevity and safety of RCC arch dams.

Keywords: Roller-compacted concrete (RCC) arch dam; Anti-cracking design; Induced joint; Equivalent strength theory; Contact unit simulation

1 Research Background

The advent of the first RCC dam in China marked a significant turning point, subsequently witnessing a rapid increase in the construction of new dams predominantly utilizing RCC technology (refer to Figure 1). As of December 2018, data from the MD&A RCC dam database indicates the construction or ongoing construction of 189 RCC dams in China, encompassing 135 gravity dams, 8 gravity arch dams, and 46 thin arch dams [1]. The design strategies commonly integrate the use of transverse and induced joints, aiming for a synergistic effect to prevent crack formation, drawing upon the distinct structural characteristics of each joint type. Despite these efforts, challenges persist in engineering practice, where many induced joints in RCC arch dams either fail to open or cracks manifest at locations devoid of induced joints. This discrepancy between design expectations and practical outcomes, including unintended negative effects, is often attributed to the sub-optimal arrangement of induced joints [2]. The complex, variable, and dynamic nature of thermal stress in RCC arch dams necessitates a design for crack prevention that accurately mirrors the dam's operational conditions from its construction phase to its functioning stage [3].

Cracking in induced joints is fundamentally a 3D fracturing problem [4]. The field has seen significant scholarly contributions [5–7]; however, the intricacies of fracture mechanics analysis via numerical methods impose constraints, particularly in executing refined calculations of stress and stress intensity factors in induced joints during complete

process simulations of RCC arch dams. An alternative approach involves conceptualizing induced joints using 3D contact element simulation and adopting an "equivalent strength" as the criterion for destruction.
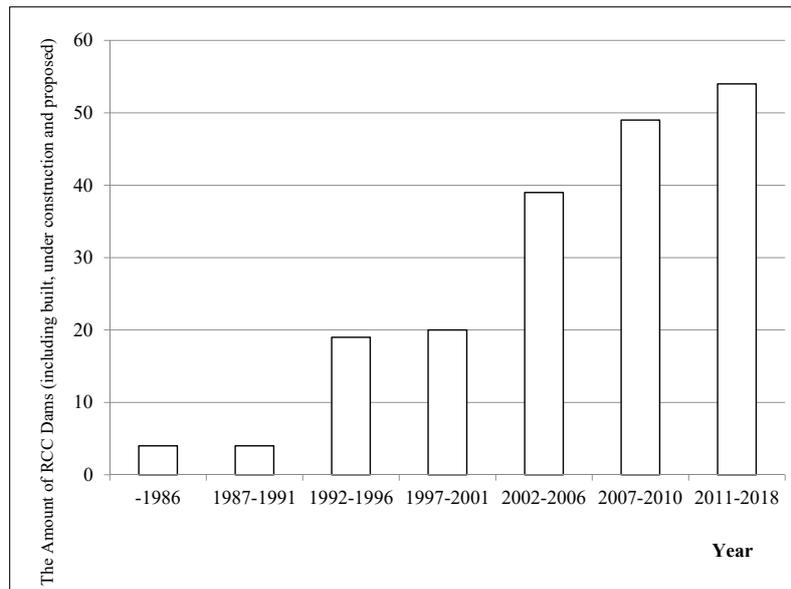

Figure 1. Trend of quantity growth in China's RCC dams

This paper delves into the actual behavior of induced joints in Chinese RCC arch dams, examining their stress distribution characteristics and evolution within the dam structure. The study employs a contact unit simulation approach with an open/close iterative function for representing induced and transverse joints in RCC arch dams. Utilizing equivalent strength theory as a basis for destruction criterion, and conducting a comprehensive process simulation of the dam, emerges as an effective method for devising joint configurations aimed at crack prevention in RCC arch dams. Subsequent to these simulations, the research further explores the joint arrangements within the dam (including the height of the bottom surface of the joints and their location) and the joint structures (encompassing induced joints, transverse joints, or a combination thereof; and the proportion of the area weakened by induced joints). Such an approach ensures the optimal opening of induced joints in line with design expectations, facilitating the release of tensile stress caused by temperature reductions and thereby assuring high-quality construction of the dam's concrete body.

2   Analysis of Factors Impeding the Opening of Induced Joints in RCC Arch Dams

The initiation of induced joints was first observed in gravity dams and subsequently employed in gravity arch and thin arch dams. In gravity dams, their primary function is to direct crack formation and alleviate thermal stress. In arch dams, these joints serve not only the aforementioned functions but also play a crucial role in force transmission while mitigating stress. However, in practical engineering applications, it has been noted that many induced joints in RCC arch dams fail to open, with crack formations occurring in areas devoid of such joints. For instance, in an RCC arch dam located in Southwest China, cracks developed in the dam body before water storage, despite the presence of induced joints (see Figure 2). This phenomenon indicates a failure to meet design expectations in inducing crack formations near the joints and also leads to additional detrimental effects. Based on the observed behavior of induced joints in domestic RCC arch dams, the inability of these joints to open concurrent with crack formation in the dams can be attributed to the following factors.

The primary factor contributing to the ineffective performance of induced joints is their misplacement. Specifically, these joints are not situated at the points of maximum stress within the dam. The thermal stress experienced by an arch dam during construction is intricately linked to the timeline and progression of construction activities. Variations from the designated construction plan can lead to discrepancies in the stress levels within the dam structure. Consequently, the positioning of the induced joints necessitates corresponding modifications. Therefore, the placement and spacing of both transverse and induced joints in an RCC arch dam require dynamic adjustment, taking into account the dam's geometry, material characteristics, meteorological and hydrological conditions, as well as the actual construction scenario. These adjustments should be informed by simulation analyses to ensure that the joints are located at points of maximal tensile stress, while maintaining the stress outside these areas below the concrete's permissible tensile stress threshold. This method has proven effective in preventing cracks in the dam structure and has been applied in the construction of numerous arch dams.
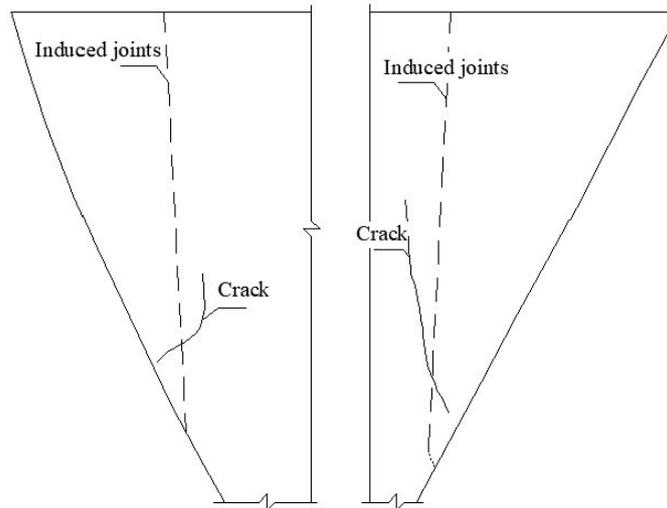
Figure 2. Downstream surface of a RCC arch dam in Southwest China

The second factor concerns the thermal stress in a RCC arch dam [8]. The construction of an RCC arch dam, in contrast to conventional concrete dams, is characterized by distinct features related to the pattern of construction joints, the temperature during arch grouting, the grouting methodology, and the methods for temperature control. These unique aspects result in the thermal stress in an RCC arch dam being markedly different from that in a conventional concrete dam. This disparity is primarily evident in the magnitude of the structure subjected to temperature-induced loading and the duration required for the temperature to decrease within the dam. Typically, the water cooling process preceding arch grouting is omitted in the construction of RCC arch dams, leading to a post-grouting body temperature higher than the dam's average temperature over several years. Consequently, the body temperature of an RCC arch dam undergoes a significant reduction following the completion of the arch structure and the commencement of water storage, inducing substantial thermal stress on the dam. However, due to hydraulic pressure, the dam predominantly remains in a compressed state, preventing full opening of the transverse or induced joints. It is only during periods of low water levels and lower temperatures that the upper portion of the dam might experience a noticeable opening, while the lower section remains compressed.

Another factor impeding the opening of induced joints is the prevailing construction methodology, which does not ensure the absence of cross slurry or running slurry in the precast of induced joints. This situation inadvertently increases the strength of the induced joints, making their opening under stress more challenging. Additionally, there is a need for improvement in the seam formation method within induced joints. By increasing the initial length of the long axis in the concrete block of an induced joint while maintaining overall strength, the likelihood of cracking within the joint can be enhanced. Of all these factors, the most significant impact arises from the improper arrangement of the induced joints.

3   Analysis of Mechanics and Numerical Computation Models for Induced Joints

The fracturing of an induced joint is fundamentally a 3D problem. Due to constraints in numerical methods for analyzing fracture mechanics, conducting detailed calculations of the complex stress and stress intensity factor of the induced joint itself during a comprehensive simulation analysis of an RCC arch dam is challenging. A practical alternative involves conceptualizing an induced joint through a 3D contact element simulation and establishing the destruction criterion based on an "equivalent strength" concept.

3.1   Mechanical Analysis Model: The Equivalent Strength Model and Its Enhancements

To investigate the cracking behavior within induced joints and to devise a rational arrangement, Professor Zeng and Ma [9] transformed the induced joint problem into two computational models: the infinite plate penetrating crack model and the elliptical crack model embedded in an infinite body (refer to Figure 3). Zhang et al. [10] have indicated that the equivalent strength models derived from these computational approaches exhibit similarities. However, the model of an infinitely large, deeply buried elliptical crack accounts for the influence of adjacent induced joints along the short axis and incorporates the effects of two critical factors: the far-field stress and the effective cracking length of the short axis in an induced joint. Consequently, most equations developed for calculating the equivalent strength of induced joints are based on this elliptical crack model, as demonstrated in Eq. (1).

$$\begin{cases} f_{eq} = \dfrac{\Phi \cdot K_{1C}}{\gamma \sqrt{\pi(a+r_0)}} \\[2mm] \gamma = \sqrt{\dfrac{2b}{\pi(a+r_0)} \tan \dfrac{\pi(a+r_0)}{2b}} \\[2mm] r_0 = \dfrac{1}{\pi}\left(\dfrac{K_{1C}}{f_t}\right)^2 \\[2mm] \Phi = \int\limits_{0}^{\pi/2} \left(\sin^2\theta + \dfrac{a^2}{c^2}\cos^2\theta\right)^{1/2} d\theta \end{cases} \tag{1}$$

(a) Calculation diagram   (b) An infinite plate penetration crack model   (c) Infinite gross buried elliptic crack model
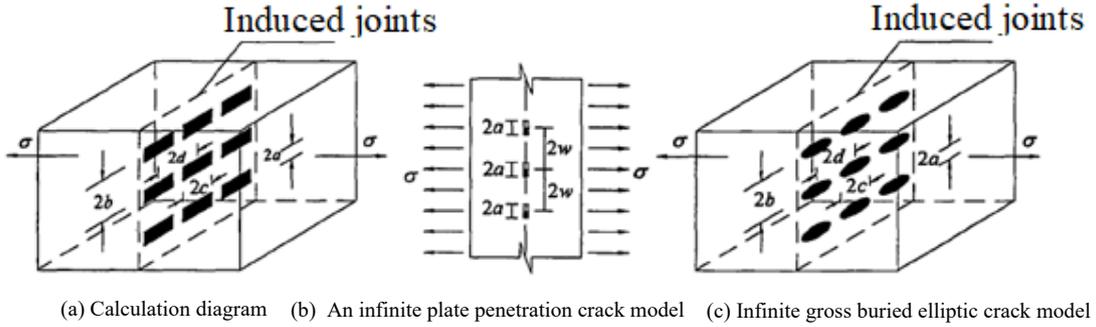
Figure 3. Calculation model of an induced joint

$$f_{eq} = \frac{\Phi \cdot K_{1C}}{\gamma \sqrt{\pi(a+r_0)}} \cdot \psi(\alpha) \tag{2}$$

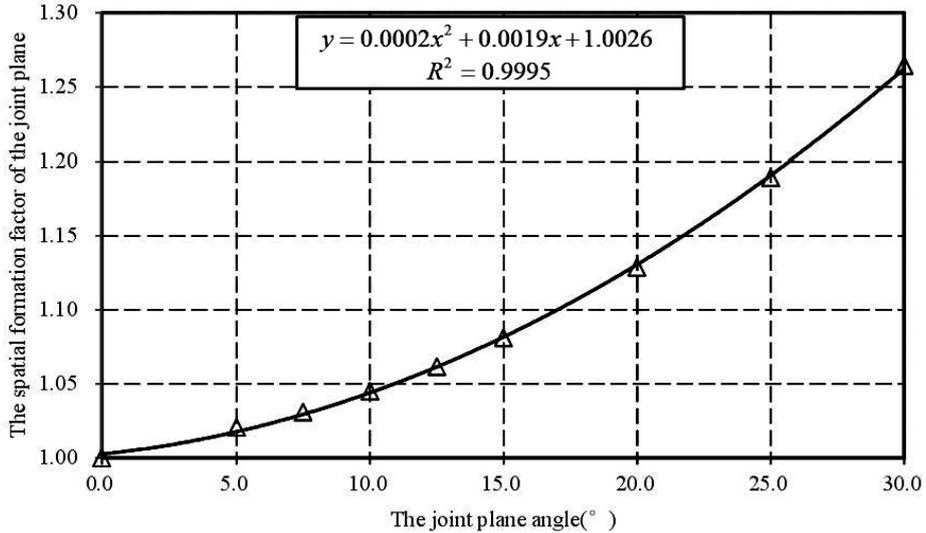$$\psi(\alpha) = 0.0002 \times \alpha^2 + 0.0019 \times \alpha + 1.0026 \tag{3}$$

Figure 4. Influence of spatial morphology on joint surface under varying joint surface angles

Numerous scholars have conducted extensive experimental research to examine the fracturing behavior of induced joints under various operational conditions, utilizing the double-K fracture theory of concrete [11–13]. These investigations have enhanced the equivalent strength theory of induced joints, considering several aspects: the type of inducing plate, the sample size effect, boundary influence, effective expansion of the crack, and the concrete's nominal fracture toughness [14–18]. However, these enhancements to the equivalent strength model for induced joints have not accounted for the spatial morphology of the crack surface. Given that cracking in an induced

joint fundamentally constitutes a 3D fracturing problem, the forces acting upon an induced joint must be analyzed considering different spatial morphologies of the crack surface. In this study, the variation trends of fracturing parameters on the crack surface under diverse loading conditions are investigated using the 3D virtual crack closure technique [19–24]. Additionally, it proposes the integration of a spatial morphology factor into the existing equivalent strength model for an induced joint [25]. This factor encapsulates the impact of the crack surface morphology, as delineated in Eqs. (2) and (3), with the corresponding relationship curve depicted in Figure 4.

3.2 Numerical Computation Model: Contact Element with Iterative Opening and Closing Function

3.2.1 3D contact surface model

From a numerical simulation standpoint, an induced joint is conceptualized as a contact plane capable of opening, closing, or slipping under external load influences. In applying numerical methods such as the finite element method for analysis, it is crucial to adopt a suitable numerical model for simulation purposes. The current analytical models for contact planes are categorized into three types [26]: (1) the equivalent continuous model, which simplifies the contact plane as a continuum and analyzes the issue using standard finite element methods; (2) modeling the structural planes as contact boundaries, whereby the mechanical behavior of these planes is simulated through various contact boundary conditions, reflecting the force-deformation characteristics of the structural plane; (3) various contact element models that represent the structural planes using specialized finite elements and boundary elements.

Considering the stress mechanics of an induced joint, prior to its opening, the concrete segments on either side of the fissure move outward and apart under tensile stress. Under compressive forces, these segments are pressed into close contact, facilitating the transmission of compressive stress. Regions devoid of fissures behave akin to regular concrete. Once an induced joint opens, the crack plane within only transmits compression or compressive shear forces, not tensile forces. In terms of the open/close status of an induced joint, it can alternate between open, closed, and slipping states under external loads. Thus, incorporating a contact boundary model based on the contact unit is essential to simulate the opening and closing behavior of an induced joint [27, 28]. This method offers a more accurate simulation of the actual operational conditions of an induced joint, particularly concerning the joint's open/close states and the transmission of shear forces by the joint.

The 3D contact surface numerical model is depicted in Figure 5.
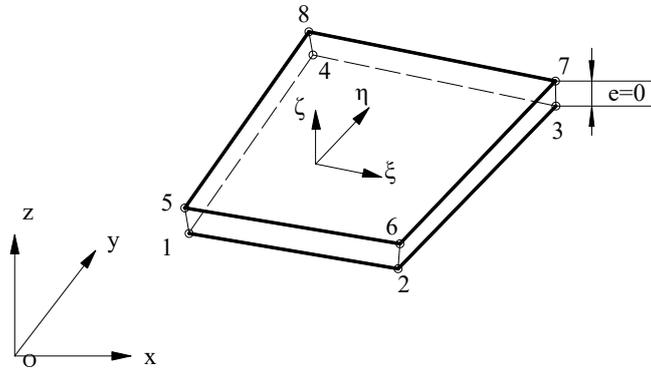
Figure 5. Schematic diagram of a 3D contact element

$$\{\sigma\} = [\lambda] \left\{ \begin{array}{c} \Delta u \\ \Delta v \\ \Delta w \end{array} \right\} + \{\sigma_0\} \tag{4}$$

$$\{\sigma\} = \left\{ \begin{array}{ccc} \tau_{xz} & \tau_{yz} & \sigma_n \end{array} \right\}^T \tag{5}$$

$$\{\sigma_0\} = \left\{ \begin{array}{ccc} \tau_{xz}^0 & \tau_{yz}^0 & \sigma_n^0 \end{array} \right\}^T \tag{6}$$

$$[\lambda] = \left[\begin{array}{ccc} \lambda_s & 0 & 0 \\ 0 & \lambda_s & 0 \\ 0 & 0 & \lambda_n \end{array} \right] \tag{7}$$

In line with the virtual work principle, the stiffness matrix of the element can be determined as outlined in Eq. (8).

$$[k^e] = \iint [N]^T [\lambda][N] dx dy \tag{8}$$

For the failure of the contact surface and subsequent crack propagation, the Mohr-Coulomb failure criterion with tension is employed. This approach entails that the contact element is deemed damaged when the normal and tangential stresses on the junction surface fulfill specific conditions: normal tensile splitting, as defined in Eq. (9), and shear failure, as specified in Eq. (10).

$$-\sigma_n \geq f_{eq} \tag{9}$$

$$\begin{cases} \tau_s = c & \sigma_n < 0, -\sigma_n < f_{eq} \\ \tau_s = c + \sigma_n \tan\phi & \sigma_n > 0 \end{cases} \tag{10}$$

3.2.2 Iterative process of opening and closing

Analysis of contact conditions

The state of the contact surface unit is determined based on the following four deformation modes:

1) Adhesion Mode: The unit remains in an adhered state prior to the occurrence of tensile and shear destruction in the contact element.

2) Slipping Mode: The unit enters a slipping state, where the upper and lower surfaces dislocate and slide relative to each other, when the contact element experiences shear destruction.

3) Open Mode: If the contact element, while in the adhered mode, is subjected to a normal stress surpassing its tensile strength, the unit undergoes expansion and destruction. Post-destruction, when the contact unit is subjected to normal tensile forces, its opening and closing are regulated by the cumulative strain. The contact unit is considered to be in an open state (i.e., open mode) if the cumulative strain is positive, indicating that the fractured unit is in a stretched condition.

4) Closed Mode: Once fractured, if the contact element exhibits a negative cumulative strain, it is in a compressed state. In such instances, the contact element is deemed to be closed (i.e., closed mode).

Under various loading scenarios, the state of the contact element aligns with one of the aforementioned four conditions, evolving in response to the prevailing stress conditions. As per the entry theory associated with general coverage contact in numerical manifold methods, alterations in the state of the contact element result in an increase in stiffness and a corresponding decrease in total force. This can be elaborated as follows:

1) Transition from Adhered to Open Mode: If a contact element transitions from an adhered state in one step to an open mode in the subsequent (n+1)th step, both the normal and tangential stiffnesses balance each other, resulting in the release of all stress within the contact element. The released stress is then treated as initial stress and transformed into node-specific loading using Eq. (11):

$$\{P\}^e_{\sigma_0} = -\int_{-1}^{1} \int_{-1}^{1} [B]^T [L]^T \{\sigma'_0\} |J| d\xi d\eta \tag{11}$$

2) Transition to Slipping Mode: In cases where the contact element remains in an adhered mode in the n-th step but undergoes shear destruction in the (n+1)-th step, the element enters the slipping mode. Consequently, a portion of the shear stress is released to the contact element, which equals to $\tau - \sigma_n \cdot \text{tg}\,\phi$. The released stress, treated as initial stress, is then converted into node-specific loading in the contact element for the next iteration cycle.

3) Closing of an Open Contact Element: If the contact element is in an open state in the nth step but transitions to a closed state under compressional force in the (n+1)-th step, both the normal stiffness and tangential stiffness need to be incorporated into the calculation.

Solution of the opening/closing iteration

The complex interactions within an induced joint can be conceptualized as a contact problem, which is inherently nonlinear. This nonlinearity stems from two primary sources: (1) The contact condition is not predetermined and evolves over time. Consequently, it must be ascertained during the resolution process. (2) The elements contributing to the nonlinearity of the contact condition include: i) The non-penetration characteristic, which prevents the contact objects from penetrating each other, ii) The normal component of the contact force, which is exclusively compressive, and iii) The frictional aspect linked to tangential contact. These specific conditions differ fundamentally from standard constraints, as they are defined by unilateral inequality constraints that exhibit significant nonlinear characteristics.

In addressing the opening and closing iterations within the contact element, the integration of a state variable into the contact model is key to addressing the efficiency issues arising from incorporating the contact plane into the

iterative calculations. This state variable is designed to document the open or closed status of the contact plane both before and after each iteration. Convergence is achieved when this state variable remains constant over successive iterations. Additionally, the rate of convergence can be substantially enhanced by forecasting the state of the contact plane and dynamically adjusting the stiffness of the spring through the plus-minus method in each iteration. These techniques significantly reduce computational overhead while ensuring the integrity of the calculation results, making them particularly effective for large-scale numerical calculations. The specific steps involved in the iterative calculation process are outlined as follows:

Step 1. Calculate the stress of each contact element and the displacement of each unit node in the i-th step.

Step 2. Determine whether the open/close condition of the contact plane will change during the i-th step:

1) For a contact element remaining in the adhered mode at the end of the $(i\text{-}1)$-th step, various outcomes are possible. If the normal stress exceeds the tensile strength, the unit is compromised by tensile stress, leading to the complete opening of the contact plane as the unit stress is released. Conversely, if the normal tensile stress is below the tensile strength threshold but the shear stress surpasses the cohesion force, the unit will still transition to a fully open state, constrained by the shear stress. In the event the normal stress is compressive and the shear stress exceeds $c + \sigma_n \tan \phi$, the adhesion at the contact plane is broken, yet the contact plane remains in a closed condition. Following the opening of the contact plane, both the normal stiffness and cohesion force are reset to zero. Should none of these scenarios occur, the contact element maintains its well-adhered state.

2) In the instance where a contact element is open at the completion of the $(i\text{-}1)$-th step, its subsequent behavior is contingent upon the type of normal stress applied. If this stress is tensile, the fissure maintains its open state. Conversely, if the stress is compressive, the opening of the contact plane will diminish. Should this opening reduce to a size smaller than a predetermined critical value, δ, the fissure is then considered closed. Upon closure, both normal and tangential stiffness are reinstated to the contact plane.

3) In scenarios where the adhesion at the contact plane is compromised but the plane itself remains closed at the end of the $(i\text{-}1)$-th step, the response of the fissure to stress is as follows: if the normal stress exerted on the contact plane is tensile, the fissure will open. Conversely, if the normal stress is compressive, the fissure remains closed.

Step 3. The unit stress is released when the contact element is destroyed. The released stress is exerted on the neighboring units as an initial stress with an inverse direction.

Step 4. Calculate the stress of the contact elements and displacements of the nodes in the $(i\text{+}1)$-th step.

Step 5. Determine if the open/close condition of the contact plane will change during the $(i\text{+}1)$-th step.

Step 6. If new changes in the condition of the contact element are found, go to step 3.

Step 7. When the open/close condition of all the contact elements remains unchanged after two steps, the iterative calculation is considered as convergence. At this moment, the open/close condition of all the contact elements is considered as the final state of the iteration calculation.

4 Study of Crack Prevention Design Using Induced Joints

4.1 Design Methods for Crack Prevention in RCC Arch Dams

The operation of RCC arch dams is characterized by distinct features when compared to traditional concrete dams. These include: (1) the ability of an induced joint to both release and transmit stress, which integrates the dam's self-weight into the load distribution on the arch and beam; and (2) the accumulation of thermal stress during construction that is not entirely released, resulting in significant residual temperature stress affecting the ultimate stress state of the dam during operation. Consequently, the design for crack prevention in RCC arch dams, particularly the design of induced joints, must accurately reflect the dam's working conditions from construction through to operation. It is essential to consider the impact of residual temperature stress on the dam's performance post-water storage, the effect of transitions between open and closed states of induced joints during the initial storage period on dam workability, and the influence of temperature loads on the safety of the arch dam after the dam body sluice storage. For RCC arch dams, determining the arrangement of different construction joints and the shape of the joint surface should be based on a complete process simulation of the entire dam, taking into account both the simulated stress during the construction period and the stress distribution during operation. The key design principles are as follows:

(1) Initially, a scenario without any joints in the dam is considered to identify not only the locations and timing of maximum stress but also to assess the reasonableness of the designed joint locations.

(2) If the locations of the construction joints are designed appropriately, the stress distribution in the dam from construction to operation will be analyzed through simulation, using the joint type specified in the design. Should the location and type of joints prove to be mismatched, the design will undergo further adjustments and re-analysis via simulation.

(3) If modifications to the design of construction joints still fail to meet the crack prevention requirements of the RCC arch dam, an increase in the number of induced and transverse joints will be considered. The design will be reassessed through simulation analysis until it fulfills the crack prevention criteria, with multiple joint arrangement plans being proposed based on the design requirements.

(4) The final joint construction plan is derived by comparing different designs. Following the selected design, a comprehensive process simulation of the dam will be conducted, encompassing self-casting, arch grouting, water storage, and long-term operation. The level of crack prevention safety will be evaluated based on the results of these simulations.

4.2 Case Study

In Southwest China, an RCC arch dam with a peak height of 141.5 meters is designated as a level-2 structure. This dam's crest measures 434.46 meters in length and 8.00 meters in width. At its base, the thickness ranges from 35 to 38 meters, resulting in an overall thickness-to-height ratio of 0.247 for the structure. Following a comprehensive process simulation of the entire dam and subsequent refinement of the original joint construction blueprint, a novel joint layout has been proposed. This revised arrangement includes two transverse joints and seven induced joints, as depicted in Figure 6. The spacing between these joints is approximately 40 meters.
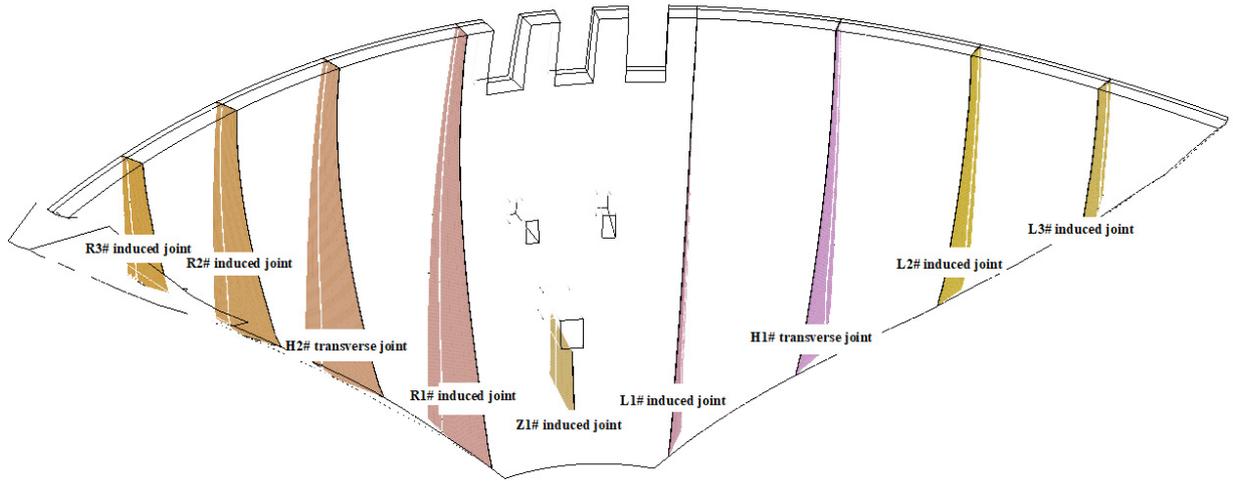

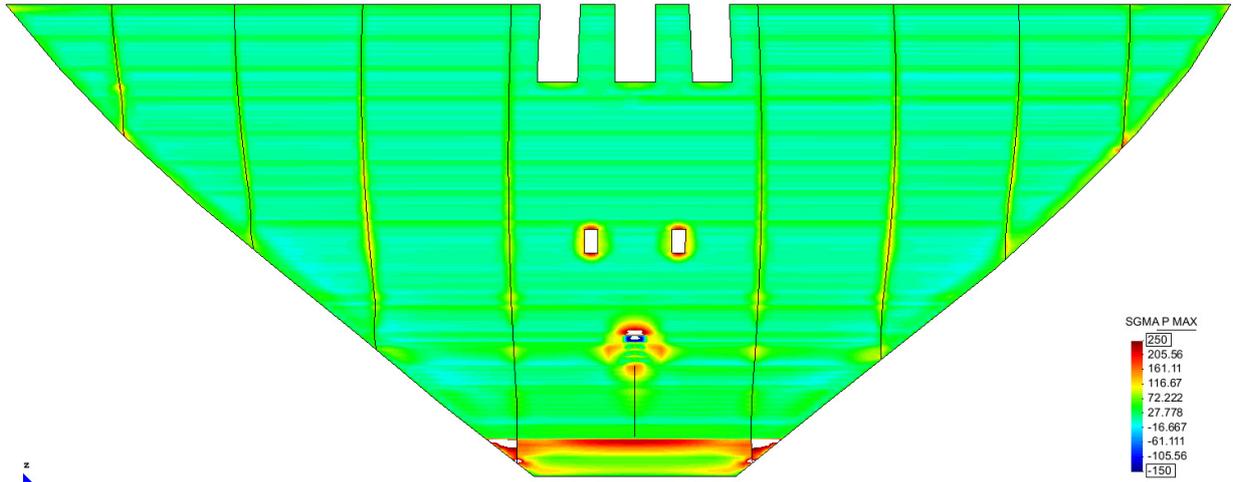**Figure 6.** Diagram of induced joint and transverse joint

Figure 7. First principal stress envelope diagram of the middle face of arch dam in late 2016 (downstream vertical vision, unit: 0.01MPa)

Based on the stress distribution cloud chart of the dam and the open/close status of the induced joints observed in the first winter before water storage, as illustrated in Figures 7 and 8, it is noted that the stress within the dam body is predominantly below the allowable tensile stress of 1.8 MPa, thereby satisfying the crack prevention criteria. However, localized exceptions are observed near the contact surface with the base, where stress concentration slightly exceeds this criterion. Prior to water storage, both transverse joints and the two induced joints nearest to the left and right dam shoulders are in a fully open state. In contrast, the remaining induced joints are partially open, with an

opening depth ranging between 2 and 5 meters. When considering both the stress distribution within the dam and the open/close condition of the induced joints, it becomes evident that the optimized joint arrangement plan effectively mitigates the excessive stress caused by hydration heat. Consequently, this strategic layout plays a crucial role in averting the development of potentially hazardous cracks in the dam body.
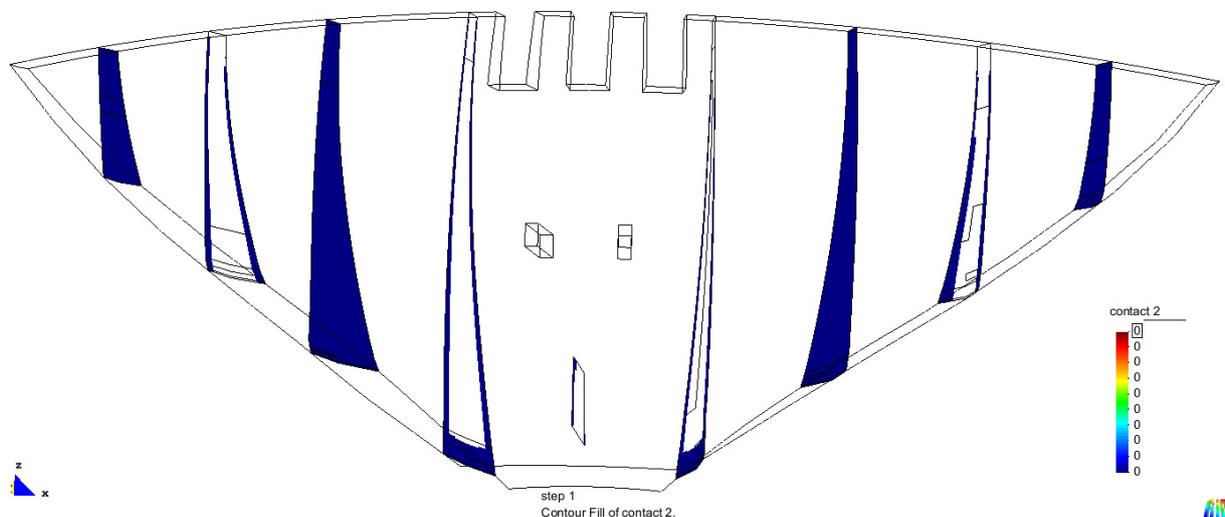

Figure 8. Distribution map of the opening and closing states of various joint surface of the arch dam in late 2016

5 Discussion on Key Issues Related to the Design of Induced Joints

5.1 Arrangement and Spacing of Induced Joints

5.1.1 Arrangement of induced joints

Induced joints are widely recognized as the most prevalent type of joints in RCC arch dams, both domestically and internationally. Their straightforward structure and ease of installation make them particularly conducive to the construction of full-section RCC dams, capitalizing on the shortened construction period typical of RCC. Nonetheless, the stress distribution within a dam featuring induced joints can exhibit significant complexity. The successful release of excessive stress, brought about by hydration heat within the dam, hinges on the complete cracking of these joints. Consequently, this process is essential for regulating the temperature of the dam and preventing the formation of cracks in the dam body.

Ensuring the opening of induced joints prior to the formation of cracks in the concrete of a dam presents a significant challenge for many dam designers. Previous research has established that the ability of induced joints to open depends on their positioning and the stress distribution within the dam. In essence, an induced joint can effectively crack and release excessive stress only if its fracture surface is subjected to sufficiently high tensile stress σ. Additionally, the ratio of this stress to the maximum tensile stress in the dam body σ_{max} should exceed the ratio of the equivalent strength of an induced joint f_{eq} to the concrete's tensile strength f_t. The most opportune moment for induced joints to fulfill their function is before the initial water storage in the arch dam. During this phase, the dam is under the stress condition of an empty reservoir, and the tensile stress caused by the cooling of hydration heat from the construction period is at its peak. Once the reservoir is filled, the tensile stress on the joint surfaces is significantly diminished due to the water's loading effect, thereby hindering the induced joints' ability to open and serve their intended purpose. Thus, the strategic placement of induced joints is crucial in determining their effectiveness in opening before the onset of crack formation within the dam.

In the design of conventional concrete arch dams, all joints within the dam body are typically transverse joints, spaced approximately 20 meters apart, with their locations remaining constant. However, for RCC arch dams, the majority of the joints are induced joints. Relying on fixed joint locations in the design and construction of these dams can lead to the failure of the joints to open, especially if there is a significant deviation from the planned construction progress. As a result, these joints may not meet the temperature control and crack prevention requirements of the dam design. Drawing from current research findings and practical engineering experiences, it is advisable to conduct a complete process simulation of the entire dam, based on the construction schedule. This simulation should calculate the thermal stress distribution in the absence of any joints. Subsequently, induced joints should be implemented at locations experiencing the maximum stress, followed by a re-calculation of the thermal stress. Through continuous adjustments to the number and positioning of the induced joints, the crack prevention requirements of the design can eventually be achieved. Moreover, if any changes occur in the construction schedule after the commencement

of the project, it is crucial to re-run the simulations and calculations based on the actual construction timeline. This process involves adjusting the locations of the joints in the yet-to-be-filled sections of the dam, continuing these modifications until the completion of the construction. This approach ensures that the induced joints effectively fulfill their intended roles in temperature control and crack prevention.

5.1.2 Induced joint + transverse joint plan

In constructing arch dams across narrow river valleys, the exclusive use of induced joints is typically sufficient. However, when dealing with wider river valleys, a greater number of joints are necessary. The sole reliance on induced joints in such scenarios carries an elevated risk, particularly concerning whether all these joints can open as intended by the design. Consequently, to ensure adherence to temperature control and crack prevention criteria, a combination of induced and transverse joints is often employed in the design. Historically, for arch dams that have already been constructed, transverse joints are generally positioned at the arch ends, where changes in tensile stress are most pronounced. This arrangement facilitates the release of localized excessive stress, aiding in meeting the temperature control and crack prevention objectives. Examples of dams utilizing this configuration include China's Shapai arch dam and Yujianhe arch dam. In recent years, there has been a shift in the placement of RCC transverse joints in dams. For RCC arch dams with a high width-to-height ratio, transverse and induced joints are commonly arranged in an alternating pattern. This means the dam is initially divided into several segments by transverse joints, with induced joints then placed between these segments. The Xiangbiling RCC arch dam in China exemplifies this design. There are also RCC arch dams that rely solely on transverse joints to ensure complete joint opening, such as the Dayakou RCC arch dam in China. It is advisable to use only transverse joints in arch dams built within narrow river valleys. In contrast, for dams constructed in wider valleys, a mix of induced and transverse joints is recommended. In these cases, transverse joints segment the dam body, and induced joints are integrated between the neighboring transverse joints.

5.1.3 Spacing between induced joints (transverse joints)

The selection of appropriate spacing for induced joints (or transverse joints) represents a significant challenge in the design of RCC arch dams. Insights drawn from the complete process simulations of several RCC arch dams in China indicate that stress variations along the arch direction are relatively minor at the arch crown's sides. Consequently, the joint spacing in these areas can be relatively large. In contrast, near the arch ends, where stress changes are more pronounced, a narrower joint spacing is required. Reflecting on the RCC engineering practices in China (refer to Table 1 for detailed information), it is common to place one induced joint (or transverse joint) every 40 to 80 meters in an RCC arch dam. The precise positioning of these joints should be tailored to the dam's layout, its stress conditions, and the construction circumstances. Additionally, care must be taken to ensure that the spacing between joints is not excessively wide, as this could lead to crack formation within the dam structure.

Table 1. Some built RCC arch dam (in China) slitting's features

Name	Location	Maximum Dam Height/m	Arc Length at Crest/m	Number of Joints	Type of Joints	Maximum Length of Slit Section/m
Xibing	Fu Jian	63	93	5	5 stress release short joints	
Puding	Gui Zhou	75	195.65	4	2 induced joints+2 transverse joints	80
Wenquanbao	Hebei	48	187.87	5	2 induced joints+3 transverse joints	34.4
Longshou	Gansu	80	140.8	4	2 induced joints+2 transverse joints	65.4
Shapai	Sichuan	130	250.3	4	2 induced joints+1 transverse joint	69.7
Shimenzi	Xinjiang	109	169.3	4	4 stress short joints+1 transverse joint	80
Linhekou	Shanxi	96.5	311.0	8	5 induced joints+3 transverse joints	49.33
Zhaolaihe	Hubei	107	198.05	4	4 induced joints	76.98
Dahuashui	Guizhou	134.5	198.43	4	2 induced joints+2 peripheral joint	85.0
Sanhekou	Chongqing	70	234.46	4	4 induced joints	56
Weihou	Guangxi	77	271.31	4	2 induced joints+2 transverse joints	61.68

5.2 Spatial Design of Induced Joint

The spatial design of induced joints in RCC arch dams typically falls into two primary categories: radial twisted joints and vertical straight joints. These two types differ solely in their spatial geometry, as depicted in Figure 9, yet they are identical in all other respects. Both joint types exhibit equivalent levels of fracturing strength, with the only distinction being a minor variation in the path of crack expansion. Additionally, both radial twisted and vertical straight joints share the same central point at varying heights, although there is a slight difference in the angle between the joint surface and the arch crown. This variance results in a minimal change in the energy required for crack expansion in an induced joint. Numerical analyses have indicated that the difference in energy needed to expand a crack in induced joints with these two different spatial geometries is less than 5% [25]. Given that concrete is a quasi-brittle material, the energy required to initiate a crack in an induced joint must exceed that needed for crack propagation. In simulation analyses of concrete dams, only a minor difference in computational results is observed when employing these two distinct spatial geometries, which is considered to be within acceptable limits.
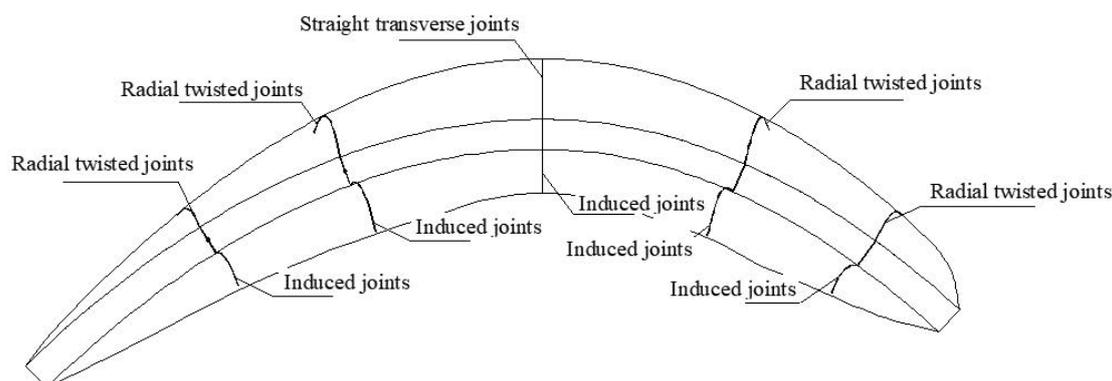

Figure 9. Diagram of spatial pattern of induced joint

In engineering practice, it's not uncommon to observe crack initiation around radially twisted induced joints or penetration through induced joints in RCC arch dams. However, similar phenomena have been noted in dams with vertical straight induced joints. The primary reason for this lies in the inherent strength of the induced joint, often a result of stringent quality control during construction. Take the Puding RCC arch dam in China as an example. This thick single-arch dam, with a height of 75 meters and a single fixed center, employs vertical straight induced joints. Post-operation, with the reservoir filled, a significant number of cracks appeared in the dam structure. Notably, a crack between the 1102-1100 m levels on the left bank, extending vertically to the base plane with a length of about 10.5 meters, penetrated through the No.3 induced joint. Such instances underscore that the spatial geometry of an induced joint does not have a significant correlation with the initiation of cracks around it or their penetration through it.

In conclusion, each spatial geometry of induced joints has its respective merits and limitations. Radially twisted joints contribute to the dam's shear strength under water loading but exhibit limited expandability and pose challenges in grouting their surfaces. On the other hand, vertical straight joints, varying in height along longitudinal and radial directions, might have a minimal impact on the dam's overall shear strength but offer better expandability and ease of grouting. Hence, selecting the appropriate spatial geometry for an induced joint largely depends on the specific conditions and requirements of the engineering project.

5.3 Spatial Design of Induced Joint

During the construction of RCC arch dams, the concrete is typically roller-compacted in layers, each with a thickness of about 30 cm. To capitalize on the rapid construction capabilities of RCC technology while simultaneously releasing the tensile stress induced by temperature loads during construction, induced joints are integrated within the dam structure. In domestic dam projects, these induced joints often follow a radial discontinuous design pattern [3], meaning they incorporate a number of gaps both horizontally and vertically. These gaps consist of custom-designed precast concrete slabs, strategically placed to facilitate the creation of multiple fissures within the same radial section of the dam. The installation of these precast concrete slabs within an induced joint is spaced at intervals of 1 to 2 roller-compacted layers vertically. Horizontally, in the radial direction, the spacing for these concrete slabs varies considerably across different engineering projects [3], leading to a significant range in the values applied. As a result, the concept of a reduced area ratio for an induced joint has been introduced. This ratio is defined as the proportion of the total void area, created by the precast concrete slabs on the surface of the induced joint, to the total surface area of the induced joint itself.
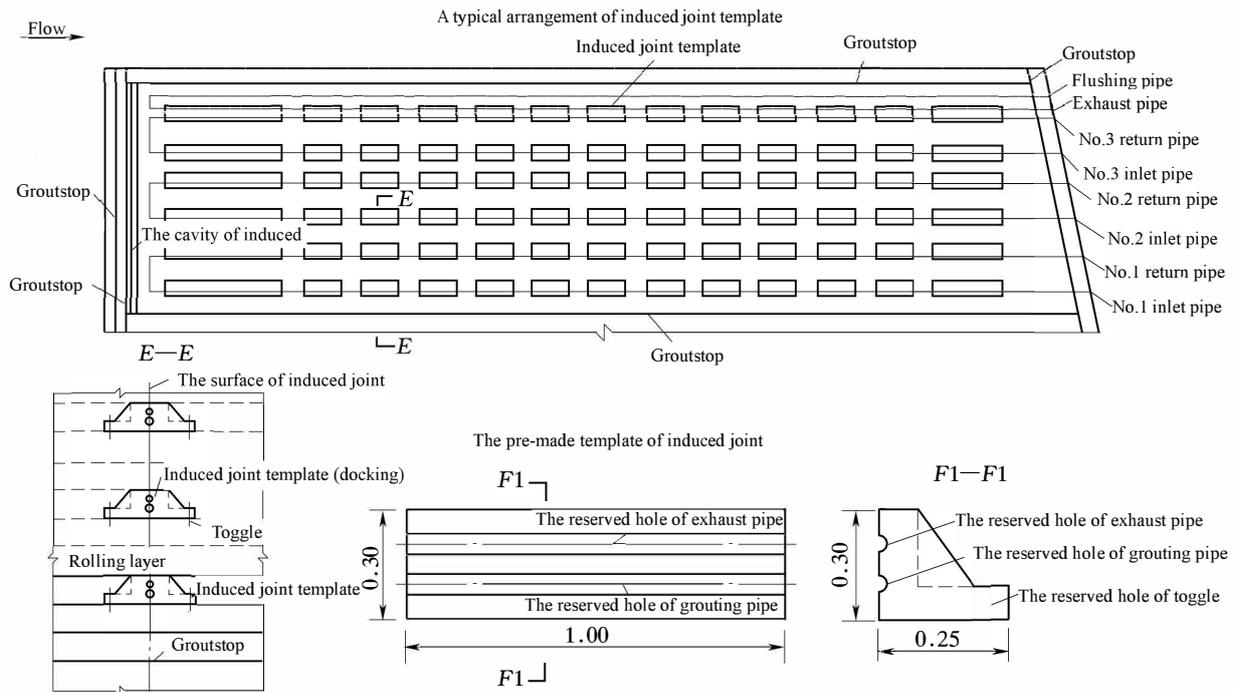
11

Figure 10. Induced joint arrangement and structure diagram

The Shapai arch dam in China is constructed using pairs of precast concrete gravity modules, as illustrated in Figure 10. Each module measures 1.0 meter in length and 0.3 meters in height. These modules are arranged in a discontinuous pattern on the joint surface in both directions, with varying lengths and spacings for the gaps along these two orientations. Specifically, in the horizontal radial direction, the gap length and spacing are 1.0 meter and 0.5 meters, respectively, while in the vertical direction (corresponding to the second roller-compacted layer), they are 0.3 meters and 0.6 meters. This configuration results in a reduced area ratio of approximately 20%. The decision to set two compacted layers as the vertical interval for placing the precast concrete slabs in the Shapai arch dam aimed to minimize the delay in overall construction progress due to the installation of induced joints. Following the construction of the Shapai dam, other RCC arch dams in China have adopted a single compacted layer as the interval for assembling these precast slabs, to diminish the strength of the induced joint. Consequently, the maximum achievable reduced area ratio does not exceed 50%.

In the design of induced joints, it's imperative that the horizontal spacing between precast concrete blocks is not set to zero. Should such spacing be nonexistent, the compacted layers devoid of precast concrete blocks would become isolated, which is undesirable given concrete's quasi-brittle nature. In concrete, crack propagation and expansion occur more readily than crack initiation. A zero spacing would mean that each compacted layer without the precast block acts as an independent concrete unit, necessitating the re-initiation of cracks. This not only presents additional challenges in initiating cracks but also complicates the control over the direction of crack expansion. Therefore, to ensure effective crack management, it's essential that all concrete on the surface of an induced joint remains connected, except at the locations of the precast concrete blocks. This connectivity allows cracks initiated within an induced joint to propagate along a predetermined path, thereby fulfilling the design requirements. Furthermore, some experts argue that placing a precast concrete block in each single compacted layer has a similar impact on overall construction progress as implementing a horizontal interval. In practical engineering applications, the latter approach is often chosen to avoid potential complications in subsequent construction phases.

In the construction of RCC arch dams, the design of precast concrete blocks for induced joints must balance construction convenience with strength requirements. These blocks should be neither too heavy nor too large. Typically, the length of a single precast concrete block in the horizontal radial direction is about 1 meter, rarely extending to 1.5 meters. To ensure the concrete on the surface of the joints forms a connected unit, except for the precast concrete blocks, the horizontal spacing between these blocks is recommended to be more than 0.5 meters. Vertically, an interval of 1 to 2 compacted layers is generally used for placing the precast concrete blocks. Consequently, the area weakened by an induced joint usually ranges from 20% to 38%. In summary, the determination of the area fraction weakened by an induced joint in an RCC arch dam design should be guided by the level of thermal stress at the joint location. A higher thermal stress necessitates a larger weakened area fraction, and vice versa. It is advisable to use an interval of one compacted layer when assembling the precast concrete blocks. Additionally,

after confirming that all the concrete on the surface of an induced joint is connected, maximizing the reduced area ratio becomes crucial to encourage crack expansion within the induced joint, aligning with the design requirements.

5.4 Summary

For arch dams in narrow river valleys, it is recommended to use only induced joints. Conversely, in wider river valleys, a combination of induced and transverse joints is suggested. Considering that each spatial pattern of induced joints has distinct advantages and disadvantages, the choice of spatial pattern should be based on the specific requirements of the project. In terms of the reduced area ratio, it is advisable to place precast concrete blocks at intervals of one compacted layer when assembling them.

6 Conclusions

Based on the analysis conducted, the following conclusions are drawn:

(1) Induced joints have emerged as a primary technique for crack prevention in RCC arch dams. Yet, it has been observed that many induced joints in these dams do not open as anticipated, and cracks sometimes form in areas without induced joints, leading to unintended negative effects. The failure of induced joints to open before the onset of crack formation is primarily attributed to their improper arrangement. Additionally, the temperature characteristics and thermal stress inherent to RCC arch dams, the prevalent construction methods, and the process of crack formation within the dam contribute to this issue. Among these, the arrangement of induced joints is identified as having the most significant impact.

(2) The fracturing of an induced joint is intrinsically a three-dimensional problem. Given the limitations of numerical methods in analyzing fracture mechanics, performing detailed calculations of the complex stress and stress intensity factor of an induced joint during a complete process simulation of an RCC arch dam poses challenges. An effective alternative is conceptualizing an induced joint through 3D contact element simulation and employing an "equivalent strength" criterion for destruction.

(3) A contact unit simulation approach, incorporating an open/close iterative function to represent both induced and transverse joints in RCC arch dams, proves effective. Utilizing equivalent strength theory as the criterion for destruction and conducting a comprehensive simulation of the entire dam enables the design of effective joint configurations for crack prevention. The simulation results facilitate further investigation into the arrangement and structure of the joints in the dam, such as height, location, and the proportion of area weakened by induced joints. This approach ensures that induced joints open as per design expectations, thereby releasing tensile stress caused by temperature reduction and maintaining high-quality construction of the dam's concrete body.

(4) In terms of joint arrangement, it is recommended to use only induced joints in arch dams constructed within narrow river valleys, while a combination of induced and transverse joints is advisable for dams in wider valleys. In the latter scenario, transverse joints segment the dam body, with induced joints placed between neighboring transverse joints. Each spatial geometry of an induced joint, possessing unique advantages and limitations, should be selected based on the specific conditions of the engineering project. For the reduced area ratio, an interval of one compacted layer is recommended when assembling precast concrete blocks. After ensuring the connectivity of all concrete on the surface of an induced joint, maximizing the reduced area ratio is crucial to facilitate crack expansion within the joint according to design requirements.

(5) Currently, an approximation approach is used for simulating induced joints. Considering the scaled-boundary finite element method's significant advantages in addressing fracture mechanics problems, future work will involve refined simulation of induced joints using this method. This advancement aims to unveil the underlying mechanisms of induced joints more accurately.

Data Availability

The data used to support the findings of this study are available from the corresponding author upon request.

Conflicts of Interest

The authors declare that they have no conflicts of interest.

References

[1] J. S. Jia, *China's Dam Construction for 60 years*. Beijing: China Water & Power Press, 2013.

[2] J. Cui, Y. F. Chen, and J. J. Tan, "Review of crack prevention technology for roller compacted concrete high arch dams," in *Proceedings of the 2014 Academic Annual Meeting of the China Dam Association*, 2014, pp. 44–50.

[3] F. P. Fan, Q. H. Long, and H. B. Luo, *Technology and Practice of Rolling Concrete Dam in Canyon Area*. Beijing: China Water & Power Press, 2015.

[4] A. J. Gu, W. X. Zhu, X. D. Wang, and D. Y. Xu, "Fracture mechanics analysis of crack director on RCC arch dam," *Hongshui River*, vol. 23, no. 1, pp. 21–24, 2004. https://doi.org/10.3969/j.issn.1001-408X.2004.01.006

[5] S. H. Yang, M. S. Cao, X. H. Ren, G. W. Ma, J. X. Zhang, and H. J. Wang, "3D crack propagation by the numerical manifold method," *Comput. Struct.*, vol. 194, pp. 116–129, 2018. https://doi.org/10.1016/j.compstruc.2017.09.008

[6] N. Sukumar, N. Moës, B. Moran, and T. Belytschko, "Extended finite element method for three-dimensional crack modelling," *Int. J. Numer. Meth. Eng.*, vol. 48, no. 11, pp. 1549–1570, 2000.

[7] A. A. Saputra, C. Birk, and C. Song, "Computation of three-dimensional fracture parameters at interface cracks and notches by the scaled boundary finite element method," *Eng. Fract. Mech.*, vol. 148, pp. 213–242, 2015. https://doi.org/10.1016/j.engfracmech.2015.09.006

[8] G. X. Zhang, B. Yang, and J. H. Zhang, "Grouting temperature and thermal load of RCC arch dam," *J. Hydraul. Eng.*, vol. 42, no. 7, pp. 812–818, 2011.

[9] Z. Y. Zeng and Q. Ma, "Study on the structural joints in the high RCC arch dam," *Water Power*, vol. 126, no. 2, pp. 32–35, 1998. https://doi.org/10.3969/j.issn.0559-9342.1998.02.011

[10] X. Zhang, Y. Song, X. Wang, and Z. Wu, "Calculation model of equivalent strength for induced crack in RCC arch dam based on double parameter fracture theory," *J. Dalian Univ. Technol.*, vol. 45, no. 2, pp. 265–271, 2005. https://doi.org/10.3321/j.issn:1000-8608.2005.02.023

[11] S. L. Xu and H. W. Reinhardt, "Determination of double-K criterion for crack propagation in quasi-brittle fracture Part I: Experimental investigation of crack propagation," *Int. J. Fract.*, vol. 98, pp. 111–149, 1999. https://doi.org/10.1023/A:1018668929989

[12] S. L. Xu, M. A. Malik, Q. Li, and Y. L. Wu, "Determination of double-K fracture parameters using semi-circular bend test specimens," *Eng. Fract. Mech.*, vol. 152, pp. 58–71, 2016. https://doi.org/10.1016/j.engfracmech.2015.12.006

[13] G. Ruiz, J. J. Ortega, C. Y. Rena, S. L. Xu, and Y. L. Wu, "Effect of size and cohesive assumptions on the double-K fracture parameters of concrete," *Eng. Fract. Mech.*, vol. 166, pp. 198–217, 2016. https://doi.org/10.1016/j.engfracmech.2016.09.001

[14] Z. Q. Huang, X. Z. Wang, X. P. Shen, and Y. P. Song, "Experiment and analysis on fracture of bilateral adjacent induced joints in RCC arch dam," *J. Hydraul. Eng.*, vol. 41, no. 2, pp. 198–204, 2010.

[15] H. C. Liu, Y. P. Song, and G. J. Yao, "Study of cracking for induced joints of shapai RCC arch dam," *J. Dalian Univ. Technol.*, vol. 44, no. 1, pp. 104–109, 2004.

[16] X. Z. Wang, Y. P. Song, X. G. Zhang, and Z. M. Wu, "Study of equivalent strength for bilateral interval crack director of RCC arch dam," *J. Dalian Univ. Technol. (China)*, vol. 46, no. 2, pp. 252–256, 2006.

[17] L. Wang, G. W. Zhang, P. Wang, and S. Yu, "Effects of fly ash and crystalline additive on mechanical properties of two-graded roller compacted concrete in a high RCC arch dam," *Constr. Build. Mater.*, vol. 182, pp. 682–690, 2018. https://doi.org/10.1016/j.conbuildmat.2018.06.101

[18] G. Liu, W. B. Lu, Y. Lou, W. D. Pan, and Z. H. Wang, "Interlayer shear strength of roller compacted concrete (RCC) with various interlayer treatments," *Constr. Build. Mater.*, vol. 166, pp. 647–656, 2018. https://doi.org/10.1016/j.conbuildmat.2018.01.110

[19] E. F. Rybicki and M. F. Kanninen, "A finite element calculation of stress intensity factors by a modified crack closure integral," *Eng. Fract. Mech.*, vol. 9, no. 4, pp. 931–938, 1977. https://doi.org/10.1016/0013-7944(77)90013-3

[20] K. N. Shivakumar, P. W. Tan, and J. C. Newman Jr, "A virtual crack-closure technique for calculating stress intensity factors for cracked three dimensional bodies," *Int. J. Fract.*, vol. 36, pp. 43–50, 1988. https://doi.org/10.1007/BF00035103

[21] M. Schöllmann, H. A. Richard, G. Kullmer, and M. Fulland, "A new criterion for the prediction of crack development in multiaxially loaded structures," *Int. J. Fract.*, vol. 117, pp. 129–141, 2002. https://doi.org/10.1023/A:1020980311611

[22] R. Krueger, "Virtual crack closure technique: History, approach, and applications," *Appl. Mech. Rev.*, vol. 57, no. 2, pp. 109–143, 2004. https://doi.org/10.1115/1.1595677

[23] P. S. Valvo, "A physically consistent virtual crack closure technique for I/II/III mixed-mode fracture problems," *Procedia Mater. Sci.*, vol. 3, pp. 1983–1987, 2014. https://doi.org/10.1016/j.mspro.2014.06.319

[24] L. Sun, D. Ma, L. Wang, X. Shi, J. Wang, and W. Chen, "Determining indentation fracture toughness of ceramics by finite element method using virtual crack closure technique," *Eng. Fract. Mech.*, vol. 197, pp. 151–159, 2018. https://doi.org/10.1016/j.engfracmech.2018.05.001

[25] H. Li, B. Li, and B. Yang, "A comparative study of the cracking effect of induced joints of various spatial formations," *Math. Probl. Eng.*, vol. 2019, 2019. https://doi.org/10.1155/2019/7876503

[26] C. H. Zhang, F. Jin, Y. L. Hou, and Y. Zhou, "Discrete-contact-fracture analysis of rock and concrete," *Chin. J. Rock Mech. Eng.*, vol. 27, no. 2, pp. 217–235, 2008.

[27] Y. Liu, G. Zhang, B. Zhu, and F. Shang, "Actual working performance assessment of super-high arch dams," *J. Perform. Constr. Facil.*, vol. 30, no. 2, p. 04015011, 2016. https://doi.org/10.1061/(ASCE)CF.1943-5509.000 0074

[28] G. Zhang, X. Li, and H. Li, "Simulation of hydraulic fracture utilizing numerical manifold method," *Sci. China Technol. Sci.*, vol. 58, pp. 1542–1557, 2015. https://doi.org/10.1007/s11431-015-5901-5

Nomenclature

The following symbols are used in this paper:

f_{eq}	equivalent strength of the induced joint;
K_{1C}	fracture toughness of concrete;
γ	correction factor that reflects the interaction between the adjacent reserved secondary joints;
r_0	concrete strain softening parameter related to the region dimensions;
Φ	the second elliptic integral;
f_t	tension strength;
θ	direction angle, starting with the long axis;
a, b, c	dimensions and interval spacing of the sub-joints shown in Figure 3;
$\psi(\alpha)$	joint plane spatial formation factor;
α	induced joint plane angle;
$\{\sigma\}$	internal stress component of the element;
$\left\{ \begin{matrix} \Delta u & \Delta v & \Delta w \end{matrix} \right\}^T$	displacement difference between two nodes on the contact surface;
$[\lambda]$	stiffness matrix;
$\{\sigma_0\}$	initial stress of the element;
λ_s	tangential stiffness coefficient;
λ_n	the normal stiffness coefficient;
σ_n	normal stress of contact surface;
τ_s	tangential shear strength of contact surface;
c	cohesion;
ϕ	frictional angle;
$\{P\}_{\sigma_0}^e$	the node load;
$[B]$	the stress -strain matrix;
$[L]$	the transformation matrix;
$|J|$	the determinant of jacobian matrix;
ξ, η	the local coordinates;